Appl. Phys. B 71, 475–480 (2000) / Digital Object Identifier (DOI) 10.1007/s003400000395

Applied Physics B
Lasers
and Optics

Broad-area diode-laser system for a rubidium Bose–Einstein condensation experiment

I. Shvarchuck, K. Dieckmann, M. Zielonkowski, J.T.M. Walraven

FOM Institute for Atomic and Molecular Physics (AMOLF), Kruislaan 407, 1098 SJ Amsterdam, The Netherlands
(Fax: +31-20/668-4106, E-mail: igor@amolf.nl)

Received: 10 April 2000/Revised version: 13 June 2000/Published online: 2 August 2000 –

Abstract. We report on master-oscillator power amplification using a broad-area laser diode (BAL) emitting at a wavelength of $\lambda = 780$ nm. The master oscillator is an injection-locked single-mode diode laser delivering a seeding beam of 35 mW, which is amplified in double pass through the BAL up to 410 mW. After beam shaping and spatial filtering by a single-mode fibre we obtain a clean Gaussian beam with a maximum power of 160 mW. There is no detectable contribution of the BAL eigenmodes in the spectrum of the output light. This laser system is employed for operation of a ^{87}Rb magneto-optical trap (MOT) and for near-resonant absorption imaging in a Bose–Einstein condensation experiment.

PACS: 42.60.By; 42.50.Vk; 32.80.Pj

Diode-laser-based systems have a profound impact on experiments in atomic physics. The excellent spectral properties and power stability make diode-lasers a highly practical tool for laser cooling and trapping experiments as well as for spectroscopic applications. The ease of operation, small size and low cost of diode-laser systems facilitate experiments in which multiple laser sources are used. These properties make diode lasers an attractive choice for experiments on Bose–Einstein condensation (BEC) of alkali systems, in particular for driving magneto-optical traps (MOTs). In BEC experiments with ^{87}Rb diode lasers are successfully used for driving the $^2S_{1/2}\,(F=2) \rightarrow {}^2P_{3/2}\,(F'=3)$ transition at 780 nm [1]. Production of a condensate usually involves a magneto-optical trap with a variety of loading schemes ranging from double-MOT systems to Zeeman slowers [2]. The drive for realising condensates with large number of particles and fast condensate production schemes has triggered the development of high-flux sources [3–5] and large optically dense MOTs (see for instance [5]). To avoid unbalanced radiation pressure in the light field, optically dense MOTs are driven by six laser beams of large diameters. The power-conserving use of three retroreflected beams is not optimal in this case. Large diameter of the beams is also important for recapture from a diverging atomic beam. Thus, the optical power required for driving a large MOT tends to go beyond the power available from single-mode diode lasers operating at 780 nm (typically not exceeding 50 mW). Alternative solutions such as Ti-sapphire lasers or diode tapered-amplifier systems provide high power but have their disadvantages aside from being expensive. The amplitude noise of an argon-ion laser-pumped Ti-sapphire laser is undesirable for many applications. Diode amplifiers with tapered waveguide offer a straightforward solution to the power limitations of narrow-bandwidth diode lasers but in practice turn out rather delicate to operate.

In this paper we report on double-pass master-oscillator power amplification with a broad-area laser diode (BAL). The advantageous properties of this system have been demonstrated and characterised in the past [6–8] and references therein], also in the context of laser cooling [9, 10]. We describe a BAL amplifier optimised for use in a ^{87}Rb BEC experiment, both for driving a magneto-optical trap and for near-resonant absorption imaging. The system operates at a wavelength of 780 nm. Using 35 mW of seeding power we obtain 410 mW of locked laser power under conditions close to power saturation. After beam shaping and spatial filtering by a single-mode fibre we obtain a clean Gaussian beam with a maximum power of 160 mW. The insertion loss of intensity modulation optics limits the available laser power to typically 135 mW under daily stable operation conditions. This allows us to trap 10^{10} rubidium atoms in a MOT loaded from a continuous slow atomic beam source [3].

1 Experimental setup

The heart of our experimental setup is a 2-W broad-area laser diode (High Power Devices Inc. HPD1120) used as a double-pass amplifier. As described in the literature, a free-running broad-area laser oscillates in multiple transverse modes which are caused by filamentation of the gain medium [11, 12]. A free-running BAL has a power spectrum with a bandwidth of the order of 2–3 nm on top of an even broader spectral background. This spectrum can

be narrowed by injecting seeding light from a narrow-bandwidth laser source. At high operating currents only part of the light emitted by the BAL can be locked. The seeding light is usually injected under a small angle as shown in the inset of Fig. 1. In this way one can suppress amplification in multiple transverse modes. Injecting at an angle also allows for an easy separation of the locked beam from the unlocked light (i.e. amplified spontaneous emission – ASE).

Our BAL-based laser system is shown in Fig. 1. The seeding laser beam is injected into the BAL at an angle of 13.5°. The amplified output beam is shaped into an approximately circular form using an anamorphic prism pair. After passing through an electro-optic modulator (EOM) it is coupled into a single-mode optical fibre, providing the laser light of high modal quality. The confocal 1:1 telescopes with the blade shutters enable us to completely shut the beam, as the extinction ratio of the EOM does not exceed 1:1000. A beam splitter in combination with an imaging lens enables us to obtain the approximation of the near and far fields of the BAL radiation. The use of a CCD camera allows continuous inspection of seeding and amplified beams in the near and far fields.

The seeding beam is focused on the front facet of the BAL in a spot of 1 μm × 90 μm[1]. This beam shaping is done with the confocal combination of a $F = 80$ mm cylindrical lens and a $f = 4.5$ mm collimator in front of the BAL (see Fig. 1). For the confocal configuration of two lenses the injection angle θ can be expressed as $\theta \approx d/f$, where d is the distance between the optical axis of the collimator and the 'optical plane' of the cylindrical lens. Translation of the cylindrical lens also causes a shift δ in position of the injection spot on the front facet: $\delta = d\,f/F$.

The locked output beam leaves the BAL at the specular reflection angle (inset in Fig. 1) and is easily separated from the unlocked light by the edge of a 45-degree deflection prism (Fig. 1). The output lobe shown in Fig. 2b is approximately 50% wider than the diffraction limit. The ellipticity of the output beam measured behind the deflection prism ranges from 3 to 5, depending on the alignment. This ellipticity is compensated by the anamorphic prism pair mentioned above.

The active area of the chip is a stripe of 1 mm length and front facet dimensions of 1 μm (height) × 200 μm (width). It is rather wide compared to most of the diodes described in the literature for similar applications [7–10], which typically are not broader than 100 μm. The front facet is anti-reflection coated (reflectivity $\leq 3\%$) whereas the back of the laser is coated for $> 99\%$ reflectivity. To a large extent the choice of the diode was based on its availability and high output power. Presently other potentially useful broad-area laser diodes are available for operation at 780 nm.

We employ a single-mode optical fibre for mode cleaning and light transport to the MOT. It is further referred to as the "output fibre". In our experience the locked BAL is far less sensitive to optical feedback as compared to a single-mode diode laser or a tapered diode amplifier[2]. We found that it is not necessary to use an optical isolator in the output beam. An

[1] We use a diffraction-limited Geltech collimator lens (Thorlabs C230TM) with 0.55 numerical aperture.

[2] We thank D. Voigt for supplying the information on tapered amplifiers.

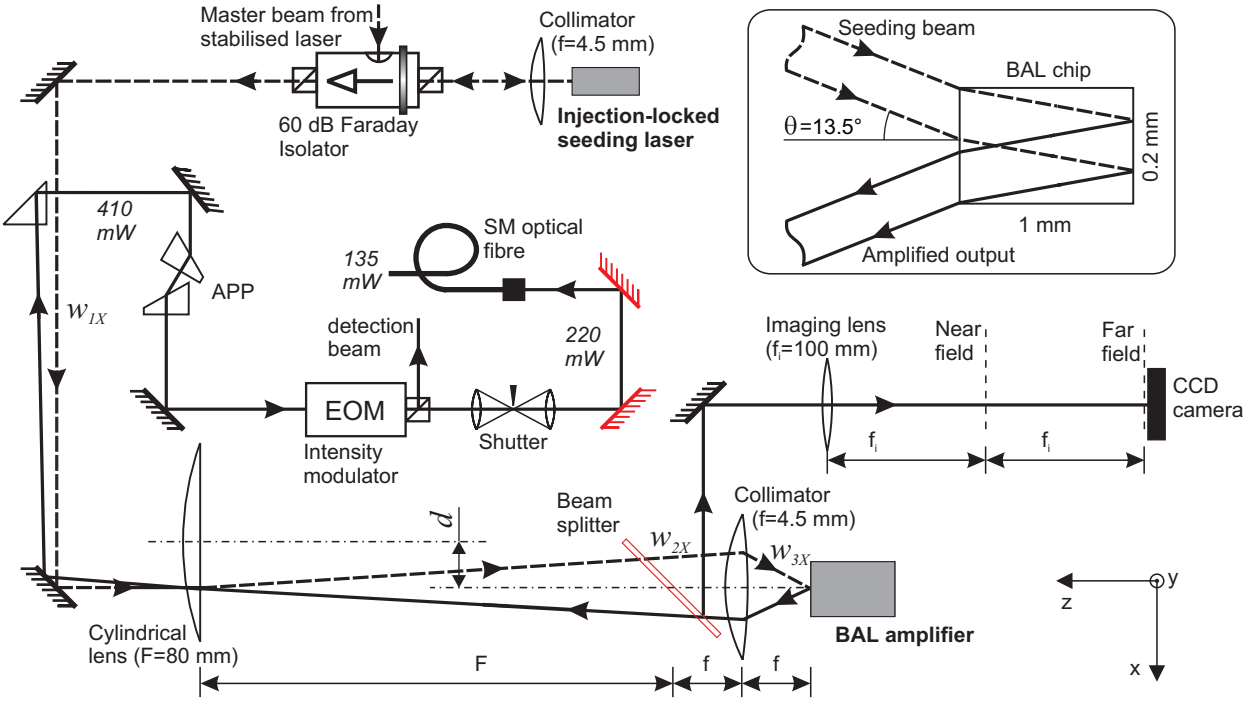

Fig. 1. Schematic diagram of the optical setup. The master beam is derived from a grating-stabilised laser not shown in the figure. The *dotted line* indicates the path of the injection beam. The *solid line* is the output of the amplifier. The numbers along the line indicate the optical power at the different stages of the beam shaping. The waist of the seeding beam, measured in the plane of the drawing, at the positions of the focal planes of the lenses is indicated by w_{1X}, w_{2X} and w_{3X} ($w_{2X} = F\,\lambda/\pi\,w_{1X}$, $w_{3X} = f\,\lambda/\pi\,w_{2X}$). Final beam shaping is done with the anamorphic prism pair (APP). The beam propagation inside the BAL is shown schematically in the *inset*

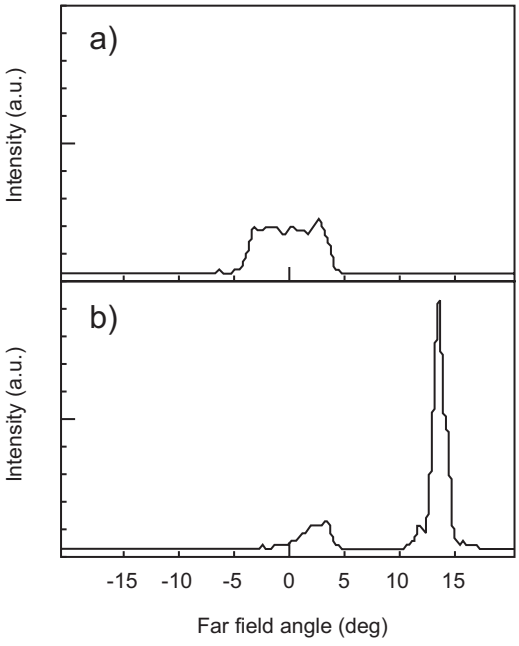

Fig. 2a,b. Far-field radiation pattern of the BAL measured along the x axis: **a** free running; **b** locked. Due to the high current of the amplifier ($I = 2.2\, I_{\rm th}$) unlocked power is visible in **b**. The intensity scales in **a** and **b** are the same

AR-coated angle-cut optical fibre with aspheric coupling lens suffices for feedback suppression.

The far-field (Fig. 2) and the near-field (Fig. 3) radiation patterns of the BAL are monitored by a CCD camera using the configuration described in [7]. This is an indispensable tool for alignment and diagnostics of the laser. The quality of the far-field pattern is an immediate indicator of successful locking. The aim is to produce a strong single lobe with minimal power in ASE[3]. As one varies the injection angle the locked pattern changes its shape, the number of lobes, and the intensity. The characteristic feature is the transfer of the power from the free-running part of the far field to the locked lobe. Monitoring of the near field is in particular important in the initial stages of alignment to establish the correct size and position of the injection spot. Figure 3 clearly shows the size and position of injection spot as well as the output beam. The near-field diagnostics is best done at zero and sub-threshold laser currents.

We have tested different injection beam spot sizes. Maximum output is obtained when the size of the seeding beam is approximately half the width of the front facet. This is in line with the reports of other groups which usually use laser diodes with less wide stripes [8, 9, 13]. The other important parameter of the system is the injection angle. This angle is controlled by a transverse shift (along x axis) of the cylindrical lens. Injection angle values reported in the literature are typically 3° to 7°. We have analysed the operation of the system for different injection angles ranging from 2° to 14°. The divergence angle of the free-running laser is 10° FWHM. Thus, one might suggest that it is best to inject the seeding beam at an angle close to 5° to match the modal pattern of the BAL. However, we found the injection angle of 13.5° to be a much better choice. For our chip geometry this angle corresponds to the situation where the seeding beam enters the BAL at one half of the front facet, travels through the chip and, after reflection from the back facet, exits on the other half of the front facet (inset in Fig. 1). Whereas the locked power is approximately the same as for the small angles, the stability of the locked lobe and sensitivity to alignment is far superior for large angles. The Fabry−Pérot effects of the BAL cavity, similar to the ones described in [9], were pronounced for injection at an angle of 6° but were not observed at 13.5°.

Our alignment procedure is similar to the one described in [9]. The seeding beam is first injected perpendicular to the front facet without using the cylindrical lens in the path, thus allowing the collimator to focus the beam directly onto the centre of the chip. The BAL current at this stage should be just above the threshold value. The coupling efficiency is now optimised by minimising the threshold current. Then the cylindrical lens is placed in front of the BAL and centred in the beam ($d = 0$). This is done by making sure that the seeding beam (visible in the near field as a much wider feature) still enters the laser in the centre of front facet. The BAL current is increased and the lens is slowly moved transversely (increasing d) to the beam, while the far field is monitored until a strong single side lobe is found (Fig. 2). At this stage the injection alignment should be fine-tuned again. This usually involves adjustment of the vertical position of the injection beam, corrections to the collimator position and small rotation of the cylindrical lens around the beam axis. Mounting the lens in a way that allows this rotation is not a critical feature of the setup but, nevertheless, provides great help in improving the coupling efficiency of the seeding beam and the shape of the output beam. Another important practical aspect of the BAL operation is the precision of z translation of the collimator lens.

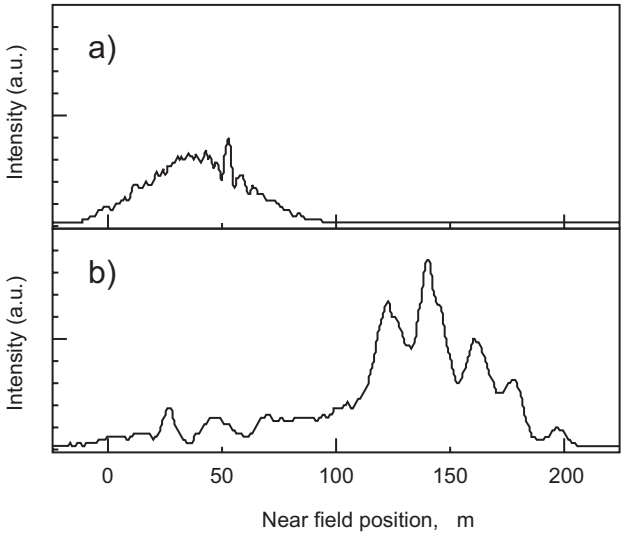

Fig. 3a,b. Details of the near field. **a** Reflection of the seeding beam from the front facet of the BAL for zero injection current ($I_{\rm BAL} = 0$ A). **b** Already below the threshold current ($I_{\rm BAL} = 0.4\, I_{\rm th}$) the output beam is clearly observed in the emission from the front facet. The intensity scales in **a** and **b** are different. Note that two beam spots do not overlap, each spot covering approximately half the facet

[3] We point out the limitations of Fig. 2 for quantitative use. In the setup depicted in Fig. 1 the output beam coming out of the collimator lens is slightly diverging in Z-X plane − coincident with the plane of polarisation. The incidence angle at the beam splitter is sufficiently close to Brewster's angle to introduce differences in reflection for different parts of the beam.

Given the performance of our BAL we need 35 mW of seeding power to satisfy our overall experimental requirements. A typical source of narrow-bandwidth laser light for laser cooling of rubidium is a grating-stabilised external-cavity diode laser [14]. The output power of such diodes rarely exceeds 50 mW for 780 nm. Thus, additional losses in the optical path of the seeding laser (for example an acousto-optic modulator and optical isolator) easily make it impossible to derive the required power from a single-mode laser diode stabilised with an external grating cavity.

To avoid limitations in seeding power we generate the seeding light in two steps. The narrow-bandwidth ($\delta\nu < 700$ kHz) master beam is produced by a grating-stabilised diode laser (TuiOptics DL100), which is locked to the signal of a Doppler-free saturation spectrometer [14]. While the main part of the output of this laser is used for other purposes in the experiment, 1 mW of light is split off and sent through a 95-MHz double-pass acousto-optic modulator (AOM). It allows us to vary the detuning with respect to the rubidium line in a range of 75 MHz. After the frequency shift in the AOM, the beam is injected into a single-mode 50-mW diode laser (Hitachi HL7851G) through the side port of the optical isolator. This injection-locked laser finally generates the seeding light for the broad-area diode.

A further advantage of this double-stage setup is related to the frequency control of the seeding light with an AOM. Even in a well-aligned double-pass AOM setup it is difficult to avoid small beam shifts occurring during large changes of the AOM modulation frequency. The BAL, which effectively acts as an amplifier, would be strongly affected by such shifts in the seeding beam in contrast to the standard injection locking of a single-mode diode chip. The intermediate laser decouples the master beam steering during the frequency change.

2 Characteristics

We have measured the emission spectrum of the locked broad-area laser behind the single-mode optical fibre. This was done with three different methods. The first method involved measuring the spectrum of the beat between the output of the locked BAL and the master laser. In the second method we measured the beat frequency of the locked BAL against an independent frequency-stabilised reference laser. This permitted observation of the spectrum of the BAL with sub-MHz resolution over a spectral range of 200 MHz. To study the spectral background of the BAL we used, as a third method, a grating spectrometer with 0.5 nm resolution.

The beat signal was obtained by mixing the output of the BAL behind the single-mode fibre with the master beam (frequency-shifted by 175 MHz using an AOM) on a photodiode (Thorlabs DET200). Figure 4 shows the power spectrum of the beat signal obtained with the spectrum analyser (Advantest R4131). The width of the spectrum is determined by the resolution bandwidth of the spectrum analyser (30 kHz). This measurement shows how closely the BAL follows the master laser.

To judge on the absolute near-resonant spectral properties of the laser system the locked output of the BAL was mixed on the photodetector with an independent reference laser. This laser was another grating-stabilised diode laser identical to the master DL100. It was frequency-locked at 160 MHz away from the master using Doppler-free satura-

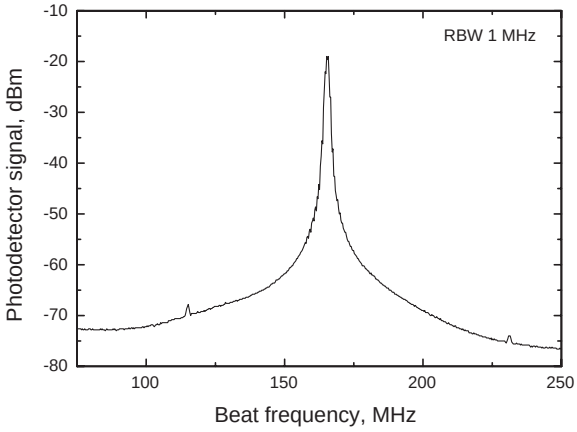

Fig. 5. Power spectrum of the beat signal between the locked BAL and the independent narrow-bandwidth reference laser (RBW 1 MHz)

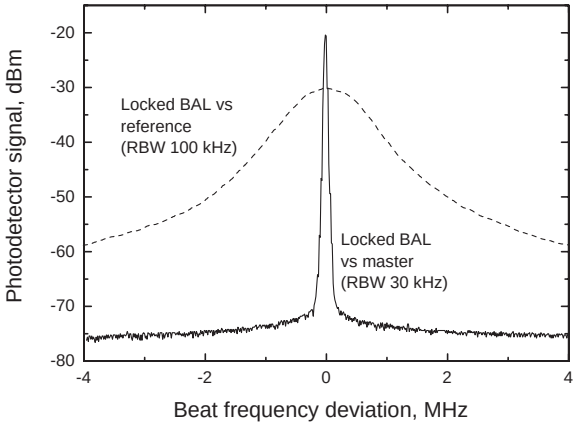

Fig. 4. *Solid line:* power spectrum of the beat signal of the locked output of the BAL with the master laser (resolution bandwidth (RBW) is 30 kHz). *Dashed line:* central feature of the power spectrum of the beat signal between the locked BAL and the independent reference laser (RBW is 100 kHz). This signal has a 3-dB bandwidth of 1 MHz

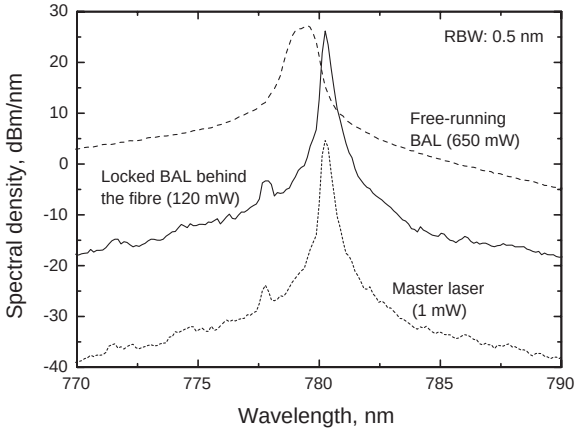

Fig. 6. Power spectra of the BAL as measured with a grating spectrometer. The spectrum of the locked BAL is observed behind the single-mode optical fibre. The spectra of the master laser and the free-running BAL are measured directly behind the lasers

tion spectroscopy. The spectrum of the beat signal is shown in Fig. 5, with its 3-dB bandwidth of 1 MHz displayed in detail in Fig. 4 (dashed line).

The spectrum measured with the grating spectrometer (Ocean Optics PC2000) is shown as the solid curve in Fig. 6. As well as the beat spectra, this measurement was done behind the output fibre. The actual 1.5-nm-wide laser modes of the free-running BAL (dashed line in Fig. 6) are not observed in the spectrum of the locked light. From this we conclude that in our setup the line shape of the output light is determined by the master laser. Note that amplification is obtained at an offset of 1 nm from the central wavelength of the free-running BAL. According to the literature the amplification bandwidth can be as large as 28 nm (FWHM) [8].

We are running the BAL amplifier at a current of 1.5 A, which corresponds to 870 mW of total optical power and 410 mW of locked power. The ASE is spatially separated from the locked output beam and is dumped in a beam-stop. Further increase of the operating current results in a relatively small increase of the locked power and mostly affects the amount of amplified spontaneous emission. This saturation behaviour is plotted in Fig. 7 and can also be seen by comparing the curves in Fig. 8. The situation is not very different with regard to saturation behaviour as a function of the seeding power (Fig. 8). One might be able increase the output power by $\approx$ 25% by doubling the seeding power. The front facet reflectivity of our BAL is $\leq$ 3%. Although we find its gain characteristics satisfactory, the research performed by other groups indicate that higher small-signal gain can be obtained, possibly with the use of the lower reflectivity coating at the front facet [6, 8, 13, 15, 16].

There is an important consideration to take into account when the BAL is run at currents close to maximum or at large seeding powers. When the broad-area laser diode is used as a double-pass amplifier, the light intensity in the region where the locked radiation is emitted is higher than that of a free-running laser. This lowers the damage threshold expressed in terms of total power of the laser output. Thus, one has to closely monitor the near-field radiation pattern when increasing the current through the laser or the seeding power. A discussion of possible damage areas on the basis of numerical modelling is given in [8]. We observed the failure of one laser diode chip by front-facet damage after running it at 2.1 A for several weeks (the maximum allowed current for HPD1120 for free-running conditions is 2.5 A).

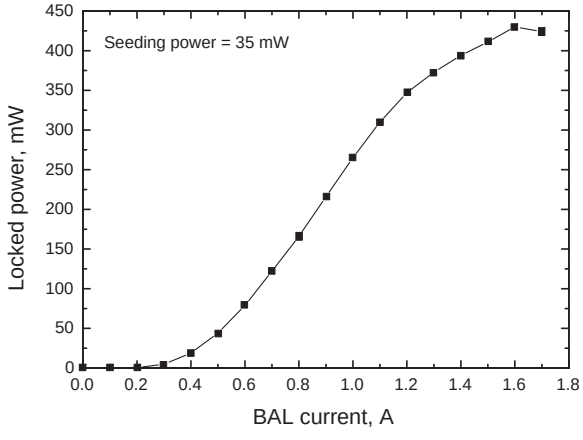

Fig. 7. The saturation behaviour of the locked power of the BAL as a function of the injection current measured for a constant seeding power of 35 mW

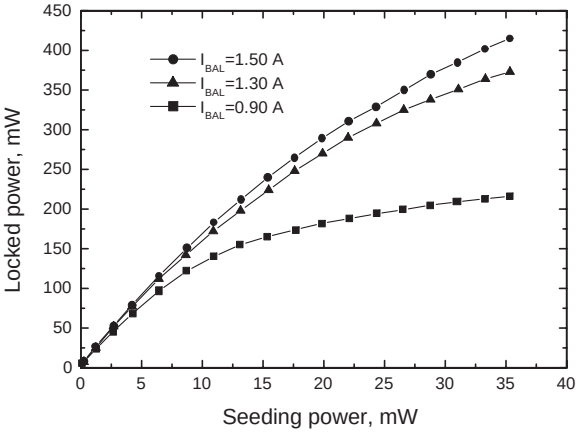

Fig. 8. Dependence of the locked power on the seeding power for different currents of the amplifier. For lower currents the saturation is reached at lower seeding power

Once the laser is aligned, it exhibits high stability of the optical power in the locked beam. We found the BAL system to be rather robust and tolerant to abuse. The system described in this paper has been proved to be reliable in daily use over the last 10 months. Its power output is comparable to the tapered amplifier systems. It also appears that the spectral properties of the amplified light are not influenced by the BAL.

We note that power requirements of the experiment did not press us to minimise the reflection losses in the beam path. When the anamorphic prism pair is used to expand the beam by a factor of 5 the reflection losses become quite large. The total losses introduced by the prism pair, further beam-shaping optics and shutter telescopes are approximately 40%. Hence, one can increase the output power by using better AR coatings[4]. A loss of $\approx$ 12% is introduced by the electro-optic modulator used for intensity control. In our present setup the total losses, including the coupling efficiency of the fibre ($\approx$ 60%), amount to approximately 67%.

3 MOT application

High optical power and good spectral properties of the light produced by the BAL make it an excellent tool for laser cooling and trapping. We use this system to realise a large density-limited magneto-optical trap [17]. The MOT is placed in a 10^{-11} mbar ultrahigh vacuum chamber and is loaded in 10 s with up to 1×10^{10} particles from a diverging fountain of cold rubidium atoms [1]. Six laser beams with $1/e^2$ diameter of 16 mm and a peak saturation parameter of 6 overlap inside the vacuum cell and provide a large capture region. The resulting gas cloud has a spherical shape with a diameter of

[4] To minimise reflection losses one might give preference to the use of an expansion telescope made out of two AR-coated cylindrical lenses instead of an anamorphic prism air. We have tried this option with equal sucess. This solution brings reflections to minimum. However, it is less flexible and compact than the anamorphic prism air.

typically 8–9 mm. Using the same beams the gas is further cooled to 40 μK in optical molasses. For this large number of atoms the temperature is mainly limited by the multiple scattering of light [18]. The cold cloud is then recaptured in an Ioffe-quadrupole magnetic trap. After adiabatic compression and evaporative cooling we reach Bose−Einstein condensation with 10^7 particles at the transition point.

The BAL-system is further used for (near-) resonant absorption imaging of atomic clouds to determine temperature, density and the number of atoms. For this application high optical power is not an issue. The detection beam is easily derived from the second output port of the EOM (see Fig. 1) and coupled into an additional single-mode fibre. As the spectral properties of the locked output of the BAL do not differ noticeably from those of the master laser, the use of the BAL does not result in loss of accuracy in imaging measurements. The detection light conveniently becomes available whenever the main MOT beams are switched off. Thus, this solution eliminates the need for an additional detection laser.

4 Summary

We have developed a robust diode-laser-based laser system producing 160 mW of narrow-linewidth light in a clean Gaussian mode. The spectral properties of the system are limited by those of the master laser which makes it suited for spectroscopic applications. The performance characteristics make it a good choice for laser-cooling experiments, allowing us at the same time to avoid drawbacks connected to alternative solutions such as a tapered waveguide diode amplifier or a Ti-sapphire laser. The laser system was successfully used for running a large MOT, sub-Doppler laser cooling and has been applied to absorption imaging of cold atomic clouds stored in magnetic traps.

Acknowledgements. We gratefully acknowledge help of K.A.H. van Leeuwen and A.C. Fey-den Boer, as well as very useful discussions with R. Spreeuw and D. Voigt. We thank L. Hillis of HPDI for his help at the different stages of this project. We also thank M. v.d. Mark and A. Valster of Philips Research for their assistance at the beginning of the project.

This work is part of a research program of the Stichting voor Fundamenteel Onderzoek der Materie (FOM), which is a subsidiary of the Nederlandse Organisatie voor Wetenschappelijk Onderzoek (NWO). K.D. was supported by a Marie Curie Research Training Grant of the Training and Mobility for Researchers (TMR) activity under the fourth European Community Framework Program for research and technological development.

References

1. M.H. Anderson, J.R. Ensher, M.R. Matthews, C.E. Wieman, E.A. Cornell: Science **269**, 198 (1995)
2. Proceedings of the International School of Physics “Enrico Fermi”, Course CXL, ed. by M. Inguscio, S. Stringari, C.E. Wieman (IOS Press, Amsterdam 1999)
3. K. Dieckmann, R.J.C. Spreeuw, M. Weidemüller, J.T.M. Walraven: Phys. Rev. A **58**, 3891 (1998)
4. Z.T. Lu, K.L. Corwin, M.J. Renn, M.H. Anderson, E.A. Cornell, C.E. Wieman: Phys. Rev. Lett. **77**, 3331 (1996)
5. W. Ketterle, D.S. Durfee, D.M. Stamper-Kurn: In Proceedings of the International School of Physics “Enrico Fermi”, Course CXL, ed. by M. Inguscio, S. Stringari, C.E. Wieman (IOS Press, Amsterdam 1999)
6. L. Goldberg, D. Mehuys, M.R. Surette, D.C. Hall: IEEE J. Quantum Electron. **QE-29**, 2028 (1993)
7. G. Abbas, S. Yang, V.W.S. Chan, J.G. Fujimoto: IEEE J. Quantum Electron. **QE-24**, 609 (1988)
8. E. Gehrig, B. Beier, K.-J. Boller, R. Wallenstein: Appl. Phys. B **66**, 287 (1998)
9. A.C. Fey-den Boer, H.C.W. Beijerinck, K.A.H. van Leeuwen: Appl. Phys. B **64**, 415 (1997)
10. M. Praeger, V. Vuletic, T. Fischer, T.W. Hänsch, C. Zimmermann: Appl. Phys. B **67**, 163 (1998)
11. H. Adachihara, O. Hess, E. Abraham: J. Opt. Soc. Am. B **10**, 658 (1993)
12. R.J. Lang, D. Mehuys, A. Hardy, K.M. Dzurko, D.F. Welch: Appl. Phys. Lett. **62**, 1209 (1993)
13. T. Pawletko, M. Houssin, M. Knoop, M. Vedel, F. Vedel: Opt. Commun. **174**, 223 (2000)
14. K.B. MacAdam, A. Steinbach, C. Wieman: Am. J. Phys. **60**, 1098 (1992), and references therein
15. L. Goldberg, M.K. Chun: Appl. Phys. Lett. **53**, 1900 (1988)
16. L. Goldberg, J.F. Weller: Appl. Phys. Lett. **58**, 1357 (1991)
17. K. Lindquist, M. Stephens, C. Wieman: Phys. Rev. A **46**, 4082 (1992)
18. C.G. Townsend, N.H. Edwards, C.J. Cooper, K.P. Zetie, C.J. Foot, A.M. Steane, P. Szriftgiser, H. Perrin, J. Dalibard: Phys. Rev. A **52**, 1423 (1995)